14B.6

PASSIVE MICROWAVE REMOTE SENSING OF TROPICAL CYCLONES

Ian S. Adams,* Michael H. Bettenhausen, and Peter W. Gaiser
Naval Research Laboratory, Washington, District of Columbia

1. INTRODUCTION

Passive microwave radiometers have a strong heritage of instruments: the Special Sensor Microwave Imager (SSM/I), the Tropical Rainfall Mapping Mission (TRMM) Microwave Imager (TMI), the Advanced Microwave Scanning Radiometer–Earth Observing (AMSR-E) and the Special Sensor Microwave Imager/Sounder (SSMI/S). These instruments measure vertically and horizontally polarized brightness temperatures over a range of frequencies to retrieve parameters such as water vapor, sea-surface temperature, cloud liquid, rain, and near-surface ocean wind speed.

The advent of microwave polarimetry offers the additional capability of passively measuring wind direction. WindSat, launched aboard Coriolis January 6, 2003, is the first satellite-based polarimetric radiometer (Gaiser et al. 2004). By measuring the full Stokes vector at 10.7, 18.7, and 37.0 GHz (as well as vertical and horizontal polarizations at 6.8 and 23.8 GHz), WindSat retrieves near-surface ocean vector winds, along with water vapor, sea-surface temperature, cloud liquid, and precipitation.

Since aircraft reconaissance flights of tropical cyclones are only deployed for systems that approach the east coast of the United States, direct satellite-based near-surface wind vector measurements offer a vital data source for monitoring the genesis of tropical cyclones (TCs). Space-based scatterometer passes only occur, at a minimum, every 12 hours. WindSat supplies much need coverage of ocean wind vectors, complementing space-borne scatterometers.

This paper presents retrievals from the current WindSat Environmental Data (EDR) processing algorithm. The retrievals are an improvement on the algorithm described by Bettenhausen et al. (2006), and are produced at a new high resolution of 25 km by 35 km. In Section 2, each of the WindSat retrievals is discussed. Section 3 presents wind vector retrievals for Hurricane Fabian along with a coincident H*Wind analysis. WindSat and H*Wind winds are compared to show the strengths of the WindSat vector retrievals and to show that WindSat offers complementary wind vector coverage to the data that are assimilated into H*Wind.

*Corresponding author address: Ian S. Adams, Code 7223, 4555 Overlook Ave. SW, Washington DC, 20375; e-mail: ian.adams@nrl.navy.mil

2. PASSIVE MICROWAVE POLARIMETRY

By measuring the electromagnetic energy radiating away from the Earth over a range of frequencies, satellite-based passive microwave radiometers provide brightness temperature (T_b) data which can be resolved into a number of atmospheric and surface products. The polarization characteristics of the measured radiation are fully described by the Stokes vector (Mishchenko et al. 2005)

$$\begin{bmatrix} I \\ Q \\ U \\ V \end{bmatrix} = \begin{bmatrix} \langle E_v E_v^* + E_h E_h^* \rangle \\ \langle E_v E_v^* - E_h E_h^* \rangle \\ -2\mathrm{Re}\langle E_v E_h^* \rangle \\ 2\mathrm{Im}\langle E_v E_h^* \rangle \end{bmatrix}. \quad (1)$$

The first two components of the Stokes vector are the sum and differences, respectively of the horizontal and vertical polarizations which have traditionally been used to retrieve water vapor, cloud, precipitation, sea-surface temperature (SST) and near-surface ocean wind speed. Unambiguous retrieval of wind direction requires the consideration of cross-correlations of the horizontal and vertical polarizations, namely the U and V components of the Stokes vector. At each of the polarimetric frequencies, WindSat measures the full Stokes vector using three feed horns: a vertical/horizontal (v/h) horn to resolve I and Q, a ±45° horn for U, and a left- and

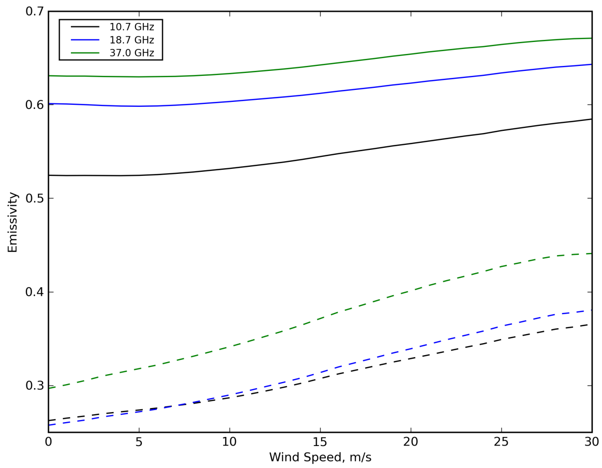

Figure 1: Sea surface emissivity as a function of wind speed for 10.7 GHz, 18.7 GHz, and 37 GHz. Solid lines denote vertical polarization, dashes represent horizontal polarization. The slope of the emissivities for 10.7 and 18.7 GHz show measureable sensitivity to high wind speeds.

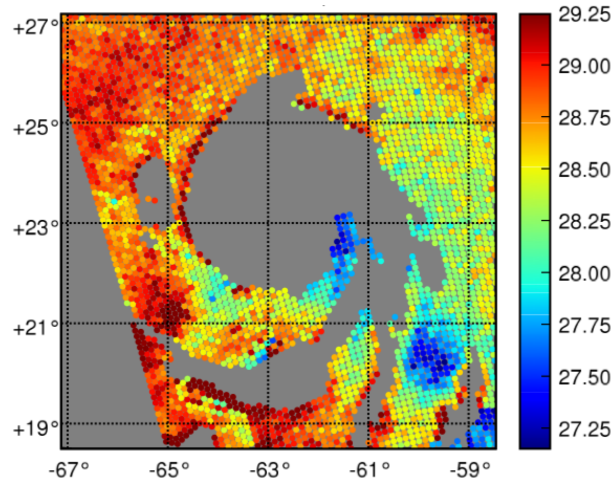

Figure 2: Sea-surface temperature for Hurricane Fabian, 2147 UTC 2003 September 03. Rain-flagged pixels have been removed from the image; however, some rain contamination is present at the edges of the flagged regions. Cold water resulting from mixing of the sea is visibly apparent in the SE corner of the TC.

right-hand circular horn (lhc/rhc) to resolve V.

The T_b measured by a space-borne instrument is a combination of downwelling radiation (atmospheric emission and space background) refected by the Earth's surface, the emission at the Earth's surface, and the upwelling emission of the atmosphere. Additionally, at microwave frequencies, the radiation propagating through the atmosphere is absorbed by gasses and absorbed and scattered by particles such as hydrometeors. These complex interactions of microwaves with the atmospheric and surface constituents, as well as the highly variable physical processes, makes geophysical retrievals in TCs difficult. This section will elucidate these challenges with an overview of surface and atmospheric physics, their radiative transfer signatures, and some additional complexities imposed by microwave radiometer instrument features.

2.1 *Surface Retrievals*

The interaction of near-surface ocean winds with the ocean surface allows for the retrievals of ocean vector winds. Wind flowing over the ocean roughens the surface. As wind increases, the surface becomes rougher, and the structure of this roughness is preferential to wind direction. The surface model currently used for WindSat vector retrievals is a form of the two-scale approach (Johnson 2006) to which an empirical correction is added to match satellite observations. The two-scale model partitions the sea surface into "long" and "short" wave regions. The short waves are distributed over the long waves. Unfortunately, in the high wind conditions of tropical cyclones, these approximations break down due to the shearing of wave crests and the spashing of breaking waves. Increased winds also result in increased foam coverage. These effects all raise the surface emissivity, i.e., the percentage of the ocean surface temperature that is sensed by an observing instrument. While such a chaotic environment is difficult to model, the increase in surface emissivity equates to a larger radiometric intensity signature from the surface. Figure 1 shows the emissivity dependence on wind speed for three WindSat frequencies: 10.7 GHz, 18.7 GHz, and 37 GHz. While the plots only display the dependency on wind speed up to 30 m/s (just below tropical storm strength), the emissivity values, with respect to wind speed, show a considerable positive slope, predicting radiometric sensitivity at high wind speeds. Wind direction retrievals are possible due to the azimuthal variation of the Stokes parameters. For Q and U the brightness temperature azimuthal variation

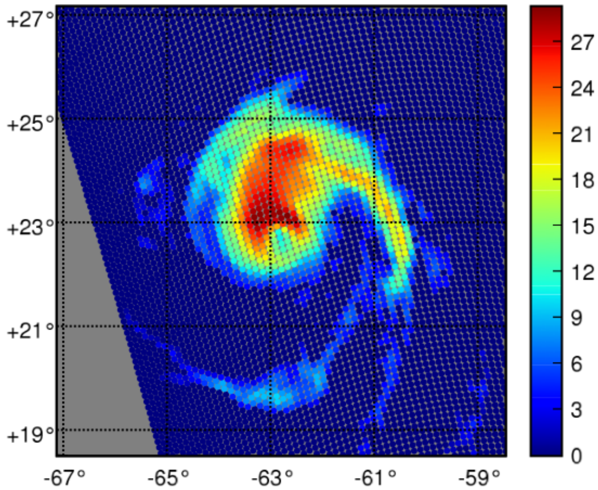

Figure 3: Surface rainfall rate retrieval Hurricane Fabian, 2147 UTC 2003 September 03.

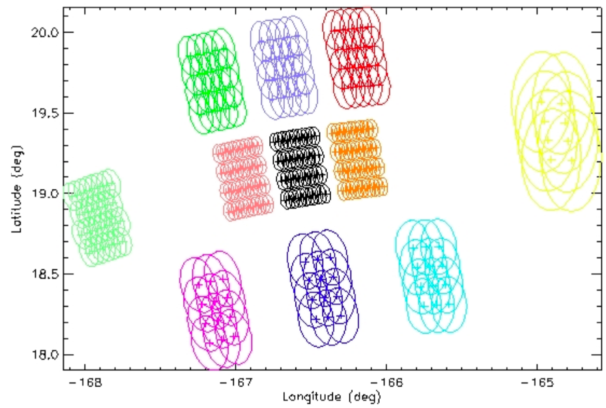

Figure 4: Projection of WindSat antenna beams on the Earth. Fields-of-view are displayed three along scan and four along track. The top row are 18.7-GHz (v/h, ±45°, rhc/lhc) projections. The center, from left to right, are the 23.8-GHz, the three 37-GHz (v/h, ±45°, rhc/lhc), and the 6.8-GHz projections. The bottom row shows 10.7-GHz (v/h, ±45°, rhc/lhc) projections.

is on the order of 1-3 Kelvin, while the variations in V peak at about 1 Kelvin.

Knowledge of SST is important for radiometric retrievals as this parameter directly correlates with the measured brightness temperature. Additionally, the SST response of is of interest to hurricane researchers, as the chaotic mixing of sea water in TCs results in the upwelling of cold water to the surface (Black and Holland 1995). Figure 2, the sea-surface temperature retrieval for Hurricane Fabian 2147 UTC, 2006 September 03, illustrates this phenomenon. The region that extends diagonally from the center of the image (storm center) to the lower right-hand (SE) corner shows noticeably lower surface temperatures.

2.2 *Atmospheric Retrievals*

Atttempting to retrieve surface parameters such as wind vectors requires proper and consitent modeling of the atmosphere. For the frequencies of concern to microwave imaging radiometers, oxygen and water vapor absorption must be considered. While oxygen mixing ratios remain constant, moderate to high water vapor levels in TC environemts can obscure surface measurements. The retrieval of water vapor, in tandem with surface retrievals, allows for the mitigation of gaseous absorption and emission.

As with water vapor and oxygen, cloud liquid water both attenuates surface signatures contributes to the atmospheric emission signal. Cloud absorption increases with frequency, affecting the WindSat 37-GHz channel the most. Unlike gas constituents, cloud cover is characterized by high spatial inhomogeneities and temporal variabilities. At microwave frequencies, however, surface retrievals in cloudy conditions are still possible.

Precipitating environments offer a unique challenge to microwave radiometry. Proper characterization and retrieval of precipitation is an extensive area of research (Simpson and Tao 1993; Kummerow and Giglio 1994). In addition to emission/absorption properties, precipitating ice and water scatter microwave radiation. The multi-frequency configuration of microwave radiometers allows for reliable retrievals of precipitation. Precipitation retrievals for WindSat, produced at 14 km resolution, are handled by a separate algorithm developed at Colorado State University and based on AMSR-E retrieval algorithm (Wilheit et al. 2003). Figure 3 presents the WindSat retrieved surface rain rates for Hurricane Fabian observation. Currently, the large signatures of precipitation preclude the WindSat EDR retreival algorithm from performing surface retreivals in heavy rain.

2.3 *Measurement Resolution and Resampling*

The high spatial variability of atmospheric liquid and ice water presents significant difficulties for accurately retrieving cloud and rain (Kummerow 1998) or for developing mitigation techniques. Traditionally, feed horns on microwave radiometers have been positioned to make concentric measurements along a single arc. To accomodate polarimetric channels, WindSat measures across three separate arcs, as displayed in Figure 4. In order to perform geophysical retrievals, the footprints must be resampled to common locations and resolutions. Retrievals in spatially inhomogeneous TC environments ideally require the highest resolution possible. Currently, WindSat processing resamples brightness temperatures to three resolutions: low, mid, and high.

3. WindSat Wind Vector Comparisons

Due to the complexities of retrieving in precipitating conditions, WindSat retrievals in precipitation are currently not considered reliable. However, the WindSat ground team has invested much effort in improving and validating wind vector retrievals in high winds. These high wind retrievals offer a valuable set of data to hurricane forecasters and analysts. To elucidate this contribution, this section presents a typical hurricane wind field retrieval and compares it with a coincident H*Wind analysis.

3.1 *H*Wind Analysis*

The H*Wind analysis system provides two dimensional wind fields of 1-minute sustained, 10-meter reference height winds by assimilating available surface, aircraft, and satellite wind data into a common framework while allowing for limited human quality control. (Powell et al. 1998) Since the 1990's H*Wind has produced products for post-storm analysis and experimental operational support. H*Wind analyses are subject to errors due to limited measurement coverage as well as instrument measurement uncertainties, and estimates of H*Wind errors range from 10% to 20%. While H*Wind is not considered truth, the analyses give the best available source of wind fields for comparison

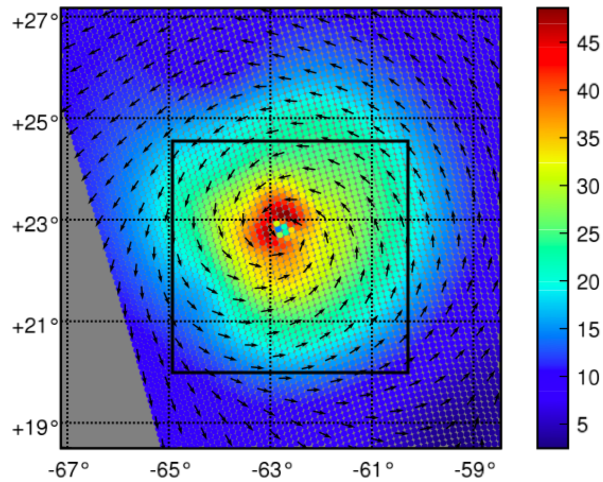

Figure 5: H*Wind analysis for Hurricane Fabian, 2147 UTC 2003 September 03. The black box denotes the region over which wind data was assimilated.

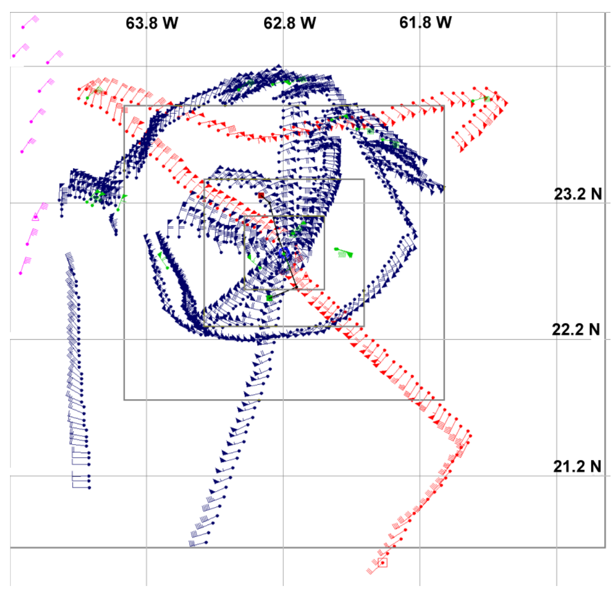

Figure 6: Assimilated data coverage for H*Wind analysis of Hurricane Fabian. The analysis includes stepped-frequency microwave radiometer (SFMR) (blue), reduced Air Force reconnaissance flight level winds (red), QuikSCAT (magenta), and GPS dropsondes (green).

with remotely sensed data.

Figure 5 an H*Wind analysis for Hurricane Fabian, Hurricane Fabian, 2147 UTC 2003 September 03. The analysis time coincides with a WindSat observation of the storm. The wind fields, normally resolved at 6 km, have been convolved with a two-dimensional gaussian antenna pattern approximation to match the WindSat retrieval resolution of 25 km by 35 km. Figure 6 shows the assimilated data coverage for the H*Wind analysis. Besides the data shown, the analysis also includes buoy and ship observations.

3.2 *WindSat Wind Field*

Figure 7 shows the WindSat retrieved wind field. The image does not contain rain flagged pixels, resulting in the gray region over the core of the storm. The flagged areas agree with the rain pattern given in Figure 3. Besides a few small issues the retrieval algorithm is well behaved. A small number of wind vectors in the field do not match the general flow of the rest of the field, indicative of an ambiguity selection issue. Also, along the edge of the rain flagged region, some pixels appear to be contaminated but not flagged which illustrates the challenges of antenna pattern resampling. When compared with the H*Wind field, most of the flow match, except for the region to the south of the storm. These data, however, fall outside of the coverage of the assimilated data, and may be the result of insufficient data in the H*Wind analysis to properly resolve the wind field. The WindSat directions in this region follow the circulation of the storm, reproducing the inflow between the rain bands.

Figure 8 is the difference between WindSat and H*Wind wind speeds. The black box shows the regions over which the H*Wind analysis assimilated data show in Figure 6. Again the wind retrieval shows well behaved wind speeds within the errors of H*Wind, not including the rain contaminated pixels, with one exception. The Windsat winds between the inner rain band and the core of the storm are low compared with H*Wind. Furthur investigation of Figure 6 shows sparse data coverage in this portion of the storm, indicating a possible problem with the H*Wind data. The winds in this band that are closer to the center of the storm do show better agreement. With respect to the assimilated data coverage, WindSat offers wind vector measurements where other data are not available.

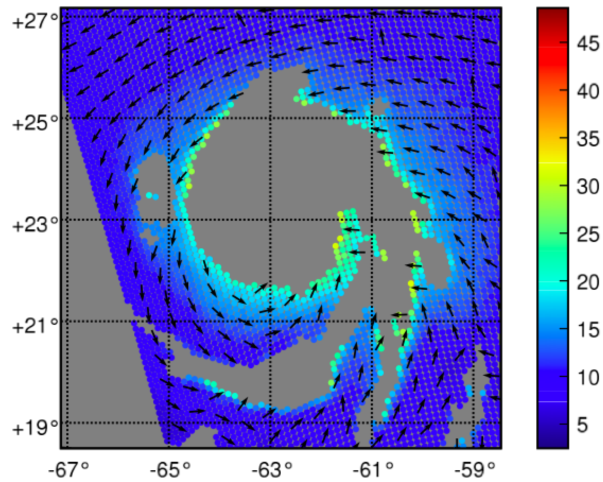

Figure 7: WindSat retrieved wind field for Hurricane Fabian, 2147 UTC 2003 September 03.

4. Conclusion

Microwave radiometers offer a range of useful products for TC forecasting and analysis. The polarimetric capabilities of WindSat offer valuable wind vector coverage over the ocean. While retrievals are currently not available in precipitation, future research should allow for mitigation in light to moderate raining conditions. Emissivity modeling confirms the radiometric sensitivity required to resolve high wind speeds.

Acknowledgments.

The authors would like to thank Christopher C. Hennon of the University of North Carolina–Asheville for providing the H*Wind analysis used in this study.

References

Bettenhausen, M. H., C. K. Smith, R. M. Bevilacqua, N.-Y. Wang, P. W. Gaiser, and S. Cox, 2006: A nonlinear optimization algorithm for WindSat wind vector retrievals. *IEEE Trans. Geosci. Rem. Sens.*, **44 (3)**, 597–609.

Black, P. G. and G. J. Holland, 1995: The boundary layer of Tropical Cyclone Kerry

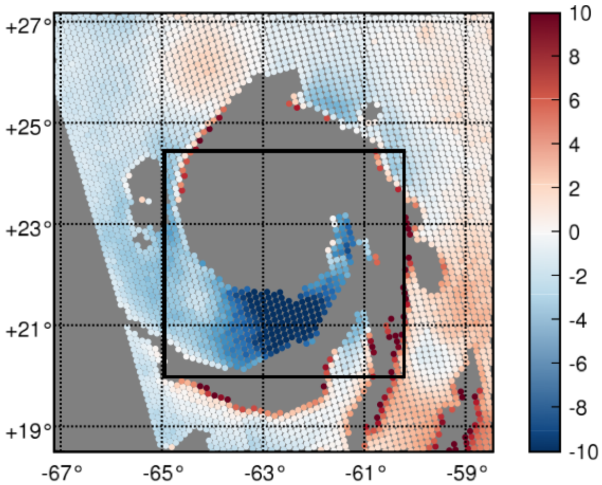

Figure 8: Difference between WindSat and H*Wind wind speeds (WindSat - H*Wind). Coverage region of assimilated data is denoted by the black box.

1979. *Mon. Wea. Rev.*, **123 (7)**, 2007–2028.

Gaiser, P. W., et al., 2004: The WindSat spaceborne polarimetric microwave radiometer: sensor description and early orbit performance. *IEEE Trans. Geosci. Rem. Sens.*, **42 (11)**, 2347–2361.

Johnson, J. T., 2006: An efficient two-scale model for hte computationof thermal emission and atmospheric reflcetion from the sea surface. *IEEE Trans. Geosci. Rem. Sens.*, **44 (3)**, 560–568.

Kummerow, C., 1998: Beamfilling errors in passive microwave rainfall retrievals. *J. App. Meteor.*, **37 (4)**, 356–370.

Kummerow, C. and L. Giglio, 1994: A passive microwave technique for estimating rainfall and vertical structure information from space. part i: Algorithm description. *J. App. Meteor.*, **33 (1)**, 3–18.

Mishchenko, M. I., L. D. Travis, and A. A. Lacis, 2005: *Scattering, Absorption, and Emission of Light by Small Particles*. NASA Goddard Institute for Space Sciences, New York.

Powell, M. D., S. H. Houston, L. R. Amat, and N. Morisseau-Leroy, 1998: The HRD real-time hurricane wind analysis system. *J. Wind Eng. Indust. Aerodynam.*, **77 & 78**, 53–64.

Simpson, J. and W.-K. Tao, 1993: The Goddard Cumulus Ensemble model. part II: Applications for studying cloud precipitating process and for NASA TRMM. *TAO*, **4 (1)**, 73–116.

Wilheit, T., C. D. Kummerow, and R. Ferraro, 2003: Rainfall algorithms for AMSR-E. *IEEE Trans. Geosci. Rem. Sens.*, **41 (2)**, 204–213.